2021 Seventh Indian Control Conference (ICC)
IIT Mumbai, India. December 20-22, 2021

Sliding Mode-Based Time-Headway Dynamics for Heavy Road Vehicle Platoon Control

K. B. Devika
Department of Engineering Design
IIT Madras
Chennai, India
devikakb@gmail.com

Shankar C. Subramanian
Department of Engineering Design
IIT Madras
Chennai, India
shankarram@iitm.ac.in

***Abstract*—Controller design for establishing string stability in Heavy Commercial Road Vehicle (HCRV) platoons usually relies on a Constant Time-Headway (CTH) policy while defining the desired intervehicular distance. However, previous studies in this area reported that CTH based design would result in string instability, while the platoon operates on certain road and vehicular operating conditions. In this regard, this paper attempts to incorporate time-headway dynamics along with vehicle dynamics to design string stable controller for HCRV platoons. Sliding Mode Control (SMC) has been suitably been utilized to derive the time-headway dynamics. The headway magnitude that are evolved from the SMC-based time-headway dynamics has been suitably integrated with an Artificial Potential Field (APF)- based string controller. Compared to CTH-based APF controller, the proposed scheme was seen to ensure string stability under wide range of operating conditions, particularly during perturbation maneuvers with high acceleration/deceleration magnitudes on low coefficient of friction roads.**

***Index Terms*—Artificial Potential Field, Heavy Commercial Road Vehicle, Platoon, String stability, Time-Headway.**

I. Introduction

The logistics sector globally is embracing new technologies to meet the increasing demand for freight transportation. Automated Heavy Commercial Road Vehicle (HCRV) platooning is one among the potential solutions that the logistic sector is currently looking froward for efficient freight movement. A heavy vehicle platoon is a convoy of trucks, which would travel very close to each other such that the overall aerodynamic drag associated with the vehicle would be minimized, leading to fuel-efficient truck operation. In addition to improved fuel economy, an automated truck platoon would result in reduced operation cost, less human resource requirement, reduced greenhouse gas emission and effective road infrastructure utilization [1]–[3].

While realizing vehicle platooning, the most important aspect that needs to be addressed is the assurance of string stability. For a platoon to be string stable, the spacing error that arises due to any perturbation should attenuate along the platoon [4]. A string stable controller is an essential component of any automated vehicle platoon framework for ensuring spacing error attenuation. String stable controller design for vehicular platoons is hence an active topic of research in the domain of automotive control [5]–[10]. Most studies in this area have utilized kinematic vehicle models for controller design. However, the authors of this paper recently established the need to include complete vehicle dynamics while designing string stable controllers for practical heavy vehicle platoons [10]. To establish string stability, it is important to maintain a desired safe spacing between vehicles in the platoon. To achieve this, most related literature used a Constant Time Headway (CTH) policy [5], [11], [12] for string stable controller design. However, while using complete vehicle dynamics-based design, it has been observed that CTH policy could not establish string stability in certain real-road operating conditions such as low coefficient of friction (μ) roads and lead vehicle perturbations maneuvers with high acceleration/deceleration magnitudes [10]. In this regard, this paper proposes a novel scheme to include time-headway dynamics in the overall platoon framework such that the headway continuously evolves with respect to time. The time-headway dynamics has been derived such that safe intervehicular spacing would be always maintained for different operating conditions. To derive the time-headway dynamics, Sliding Mode Control (SMC) has been used in this study.

Conventionally, SMC is used for the design of controllers for dynamical systems to obtain robust closed-loop performance [13], [14]. However, this paper explores the utility of SMC from another perspective, wherein it is used to derive the time-headway dynamics such that the overall platoon framework is robust to perturbations under different operating conditions. This can be considered as a novel application of SMC strategy.

The overall design framework of the proposed heavy vehicle platoon formation is shown in Fig. 1. A string stable controller is integrated with the SMC-based time-headway generation algorithm such that it would help the platoon to maintain the desired time-headway that is being evolved. An Artificial Potential Field (APF) based string stable controller for heavy vehicle platoons has been recently designed by the authors to establish string stability under different road and vehicular operating conditions. When compared to state-of-the-art string stable controller designs, this approach possesses attributes like minimum data requirement from neighboring vehicles, simple control structure and actuator-

2021 Seventh Indian Control Conference (ICC) | 978-1-6654-0978-0/21/$31.00 ©2021 IEEE | DOI: 10.1109/ICC54714.2021.9703151

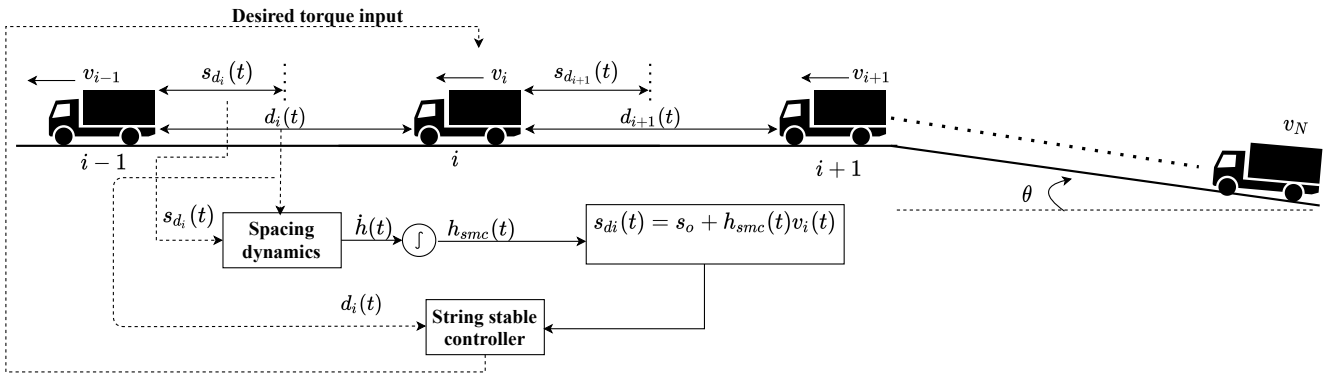

Fig. 1. Proposed platoon framework.

friendly control action. Hence, it has been used in this paper to establish string stability along with the SMC-based headway evolution algorithm.

II. Vehicle Dynamics

A platoon framework as shown in Fig. 1, with N HCRVs (1 leader and (N-1) follower configuration) has been considered in this work. The assumptions made in this study are:

- Only longitudinal vehicle dynamics has been considered in the design.
- The tyre model parameters and vehicle parameters were assumed to be known.
- Assumed equal load distribution on the left and the right wheel of a specific axle of the vehicle.

The kinematic equation that characterizes the leader vehicle in the platoon is

$$\dot{x}_0(t) = v_0(t), \tag{1}$$

where, $x_0(t)$ and $v_0(t)$ are the position and longitudinal speed of the leader vehicle, $v_0(t)$ is the speed to be followed by the follower vehicles. As presented in [10], a complete vehicle dynamics model that incorporates factors such as resistive forces, wheel slip, tyre model, wheel dynamics, normal forces and actuator dynamics has been used in this paper to characterize the follower vehicles. The position and longitudinal speed dynamics of the i^{th} follower vehicle are represented as

$$\begin{aligned} \dot{x}_i(t) &= v_i(t), \\ \dot{v}_i(t) &= \Omega(v_i(t), \tau_{ji}(t)), \end{aligned} \tag{2}$$

where, $\tau_{ji}(t)$ represents the drive/brake input with $j = f, r$, indicating front and rear wheels, respectively. Here, $\Omega(v_i(t), \tau_{ji}(t))$ represents a nonlinear function in $v_i(t)$ and $\tau_{ji}(t)$, and is given by

$$\Omega(v_i(t), \tau_{ji}(t)) = \frac{1}{m_i}\left(\sum_{j=f,r} F_{xji}(\lambda_{ji}(t), \tau_{ji}(t)) - F_{Ri}(t)\right). \tag{3}$$

Here, m_i represents the mass of the i^{th} follower HCRV and $F_{xji}(\lambda_{ji}(t), \tau_{ji}(t))$ represents the longitudinal force at the tyre-road interface. The longitudinal force is a function of the longitudinal wheel slip ratio, $\lambda_{ji}(t)$, the friction coefficient (μ) between the tyre and the road, and the normal load on the tyre ($F_{zji}(t)$) [15]. These factors are characterized by the following equations:

$$\begin{aligned} \lambda_{ji}(t) &= \begin{cases} \frac{v_i(t) - r_{ji}\ \omega_{ji}(t)}{v_i(t)}, & \text{during braking,} \\ \frac{r_{ji}\ \omega_{ji}(t) - v_i(t)}{r_{ji}\ \omega_{ji}(t)}, & \text{during drive,} \end{cases} \\ \dot{\omega}_{ji}(t) &= \frac{1}{I_{ji}}(\tau_{ji}(t) - r_{ji}F_{xji}(t)), \\ F_{zfi}(t) &= \frac{m_i(g(l_{ri}\cos\theta - h_i\sin\theta) - a_i(t)h_i) - F_{ai}(t)\ h_{ai}}{l_{fi} + l_{ri}}, \\ F_{zri}(t) &= \frac{m_i(g(l_{fi}\cos\theta + h_i\sin\theta) + a_i(t)h_i) + F_{ai}(t)\ h_{ai}}{l_{fi} + l_{ri}}, \end{aligned} \tag{4}$$

where, r_i, ω_{ji} are the tyre radius, the angular speed of the wheels, respectively. I_{ji} is the moment of inertia of wheels, and $a_i(t)$ represents the longitudinal acceleration. The height of the C.G. of the vehicle is indicated by h_i, and h_{ai} represents the height of the location at which the resultant aerodynamic force acts. Here, l_{fi} and l_{ri}, show the longitudinal distances of the front and rear axles from the C.G. of the vehicle, respectively, and θ represents the road gradient, which is defined to be positive for an up-grade and negative for a down-grade.

In this study, the Magic Formula (MF) tyre model [16] has been used to characterize the longitudinal force at the tyre-road interface, which is given by

$$F_{xji}(\lambda_{ji}(t)) = D\sin(C\tan^{-1}(\Gamma - E(\Gamma - \tan^{-1}\Gamma))) + S_V, \tag{5}$$

where, $\Gamma = B\lambda_x(t)$, and $\lambda_x(t) = \lambda_{ji}(t) + S_H$.
The MF model parameters, B, C, D, E, S_H, S_V were obtained from the vehicle dynamic simulation software, IPG TruckMaker®.

In Eq. (3), $F_{Ri}(t)$ represents the resistive force on the i^{th} vehicle, which is given by

$$F_{Ri}(t) = -m_i g(f_i\cos\theta + \sin\theta) - \rho a_{fi} C_{Di}(t)\frac{v_i(t)^2}{2}, \tag{6}$$

where, f_i and ρ represent the rolling friction coefficient and the air density, respectively. The vehicle frontal area is represented by a_{fi} and C_{Di} indicates the drag coefficient.

The transfer function of the pneumatic brake system of an HCRV obtained via Hardware in Loop experimentation [17] is given by

$$P_{ji}(s) = \frac{\tau_{ji}(s)}{\tau_{desji}(s)} = \frac{1}{1+\tau_{dji}s}e^{-T_{dji}s}, \tag{7}$$

where, τ_{dji} represents the time constant, and T_{dji} is the time delay, and τ_{desji} and τ_{ji} indicate the demanded brake torque and actual brake torque developed, respectively. The experimentally corroborated values for this model parameters are, $\tau_{dji} = 260$ ms and $T_{dji} = 45$ ms [17], and have been utilized in this study. From literature, it can be understood that a first-order model with time constant and delay is suitable for approximating the powertrain dynamics during the acceleration/drive phase [18]. Hence, a similar model as presented in Eq. (7) has been used to incorporate powertrain dynamics during the acceleration phase.

III. Proposed Time-Headway Dynamics

A. Platoon Spacing Policy

The spacing between a pair of vehicles in the platoon at each time instant t is given by

$$d_i(t) = x_{i-1}(t) - x_i(t). \tag{8}$$

The desired inter-vehicular distance is defined as

$$s_{d_i}(t) = s_o + h_i v_i(t), \tag{9}$$

where, s_o and h_i represent standstill spacing and the time-headway respectively. The spacing error is given by

$$e_i(t) = d_i(t) - s_{d_i}(t). \tag{10}$$

B. Time-Headway Dynamics via Sliding Mode Control

The core idea is to derive time-headway dynamics in such a way that error in intervehicular spacing error is driven to zero through a sliding mode motion. For this, the sliding function is defined as

$$S_i = \eta e_i(t), \tag{11}$$

where, $\eta > 0$. Now, to derive the time-headway dynamics, a reaching law approach for SMC is used. To deal with chattering issues in conventional SMC, a Power Rate Exponential Reaching Law (PRERL) proposed in [13] has been used in this study. PRERL has been proved to possess attributes like, fast control action and robustness along with chattering mitigation [13]. PRERL is given by

$$\dot{S}_i(t) = -\frac{\psi}{\delta_0 + (1-\delta_0)e^{-\alpha|S_i(t)|^p}}|S_i(t)|^{\chi}\text{sign}(S_i(t)). \tag{12}$$

Here, $\psi > 0$ is the controller gain, $\delta_0 < 1, \alpha > 0, 0 < \chi < 0.5$ and $p > 0$ are controller parameters that affect the reaching time and chattering mitigation properties. On evaluating the first derivative of Eq. (11) and using Eq. (8), Eq. (9), and the PRERL structure given by (Eq. 12), one can write,

$$\begin{aligned}\dot{S}_i(t) &= \eta\Big(v_{i-1}(t) - v_i(t) - h_i(t)\dot{v}_i(t) - v_i(t)\dot{h}_i(t)\Big) \\ &= -\frac{\psi}{\delta_0 + (1-\delta_0)e^{-\alpha|S_i(t)|^p}}|S_i(t)|^{\chi}\text{sign}(S_i(t)),\end{aligned} \tag{13}$$

which gives,

$$\begin{aligned}\dot{h}_i(t) = \frac{1}{\eta v_i(t)}\Big[&\frac{\psi}{\delta_0 + (1-\delta_0)e^{-\alpha|S_i(t)|^p}}|S_i(t)|^{\chi}\text{sign}(S_i(t)) \\ &+ \eta(v_{i-1}(t) - v_i(t) - h_i(t)\dot{v}_i(t))\Big].\end{aligned} \tag{14}$$

This dynamics would give the real-time time-headway magnitude (represented as $h_{smc}(t)$) that needs to be used by the string stable controller while estimating the desired safe distance, $s_{di}(t)$ (as shown in Fig. 1).

IV. String Stable Controller using APF

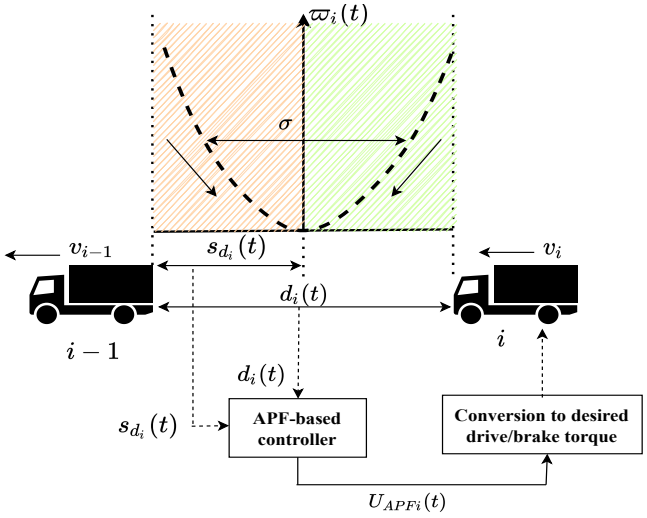

Fig. 2. APF action.

The basic schematic explaining the string stable controller design using Artificial Potential Field (APF) is shown in Fig. 2. The control objective in a string stable controller design problem is that the spacing between a pair of vehicles in the platoon should be equal to the desired safe spacing $s_{di}(t)$. In this time-headway dynamics-based approach, $s_{di}(t)$ could be written in terms of the headway magnitude evolved from the SMC-based time-headway dynamics, $h_{ismc}(t)$. Hence, the control objective can be written as

$$\begin{aligned}&d_i(t) \to s_{di}(t) = s_o + h_{ismc}(t)v_i(t), \\ &v_i(t) \to v_{i-1}(t).\end{aligned} \tag{15}$$

For string stable operation, APF acts in such a way that when, $d_i(t) > s_{d_i}(t)$, then the follower vehicle has to accelerate, and when, $d_i(t) < s_{d_i}(t)$, the follower vehicle

should apply brakes. To design such an APF, an augmented error function ($\vartheta_i(t)$) is defined as,

$$\vartheta_i(t) = \kappa e_i(t) + \dot{e}_i(t), \tag{16}$$

where, κ is a positive real number, Here, $\vartheta_i(t)$ incorporates error in both intervehicular distance and longitudinal speed. The value of $\vartheta_i(t)$ would be zero for a platoon to be string stable. On selecting a potential function, it is possible to arrive at the control inputs by finding the gradient of the potential [19].

In this study, the gradient is taken with respect to the augmented error function, $\vartheta_i(t)$. A candidate potential ($\varpi_i(t)$) of the form,

$$\varpi_i(t) = \frac{1}{2}\sigma_i \vartheta_i(t)^2, \tag{17}$$

is selected here to design the controller, where, $\sigma_i > 0$. From Eq. (17), the acceleration/deceleration control input can be obtained as,

$$u_{APF_i}(t) = \frac{\partial \varpi_i(t)}{\partial \vartheta_i(t)} = \sigma_i \vartheta_i(t). \tag{18}$$

Now, using Eqs. (7), (9) and (8) in Eq. (16), the control input, Eq. (18) takes the form

$$u_{APF_i}(t) = \sigma_i \Big(\kappa(x_{i-1}(t) - x_i(t) - s_o - h_i v_i(t)) + v_{i-1}(t) - v_i(t) - h_i \dot{v}_i(t) \Big). \tag{19}$$

This expression corresponds to the desired acceleration/deceleration component for the vehicles to maintain string stability. It can be noticed that in this approach, the control equation described by Eq. (19) depends only on the position and speed information from the preceding $(i-1)^{th}$ vehicle and the host (i^{th}) vehicle is required. Information from the succeeding $(i+1)^{th}$ vehicle is not required by the control equation. Moreover, this approach does not demand acceleration information from the $(i-1)^{th}$ vehicle. This makes the APF approach for string stable control design less information/data dependent. The total desired torque input can be obtained as,

$$\tau_{desi}(t) = m_i r_i u_{APF_i}(t). \tag{20}$$

This torque would be distributed between front and rear wheels as explained below.

During acceleration: It is assumed the vehicles are rear wheel–driven, and hence,

$$\begin{aligned} \tau_{desfi}(t) &= 0, \\ \tau_{desri}(t) &= \tau_{desi}(t). \end{aligned} \tag{21}$$

During braking: A linear torque distribution assumed between front and rear wheels, then,

$$\begin{aligned} \tau_{desfi}(t) &= \beta \tau_{desi}(t), \\ \tau_{desri}(t) &= (1-\beta)\tau_{desi}(t), \end{aligned} \tag{22}$$

where, β represents the torque distribution factor.

V. Results and Discussion

A platoon of 5 homogeneous HCRVs (one leader plus four follower configuration) has been considered. The vehicle parameters used in [10] were adopted here. From an earlier work conducted by the authors, it was found that a CTH-based APF string stable controller could ensure sting stability under a wide variety of operating conditions for lower acceleration/deceleration magnitudes ($< 2\text{m/s}^2$). However, string stability under perturbation maneuvers of higher acceleration/deceleration magnitudes were not guaranteed, particularly on roads with low coefficient of friction (μ). To address this problem, the design methodology including h dynamics has been adopted in this paper. Evaluations were performed for acceleration/deceleration magnitudes $\geq$ 2m/s^2 for a leader operating between 5 m/s and 15 m/s. Different road conditions, dry and wet, corresponding to μ values of 0.8 and 0.4, respectively, were used in the study. The test cases were simulated for $\sigma_i = \sigma$, for all the follower vehicles. Results corresponding to different sets of operating conditions have been presented in Table I.

Tracking profile		μ	String stability (without h dynamics)	String stability (with h dynamics)
Accelerating	2 m/s^2	Dry	Yes	Yes
		Wet	No	Yes
	5 m/s^2	Dry	No	Yes
		Wet	No	Yes
Decelerating	-2 m/s^2	Dry	Yes	Yes
		Wet	No	Yes
	-5 m/s^2	Dry	No	Yes
		Wet	No	Yes

TABLE I
Performance evaluation under different operating conditions

From Table I, it can be observed that the design methodology with constant h could ensure string stability only in limited scenarios. String stability was ensured only for profiles with 2 m/s^2 acceleration/deceleration magnitudes, operating on a dry road. However, if one were to include the h dynamics in the platoon design framework, string stability could be ensured for acceleration/deceleration magnitudes as high as 5 m/s^2 in both dry and wet roads.

Figure 3 presents the position profiles for a lead vehicle speed perturbation from 15 m/s to 5 m/s with a deceleration magnitude of 2 m/s^2 on a wet road. Figure 3(a) presents the position profile for a constant h (without including h dynamics) with vehicles colliding each other, causing string instability. On the other hand, the inclusion of h dynamics in the platoon design framework resulted in string stability as presented in Fig. 3(b). The corresponding speed tracking profiles are presented in Fig. 4. Using the proposed approach, good tracking performance was assured without any overshoot in longitudinal speed.

At $t = 15$ s, the lead vehicle is assumed to be braking and the speed starts decreasing. This would bring the follower vehicles closer and could result in collisions, as presented in Fig. 3(a). The inclusion of h dynamics in the platoon

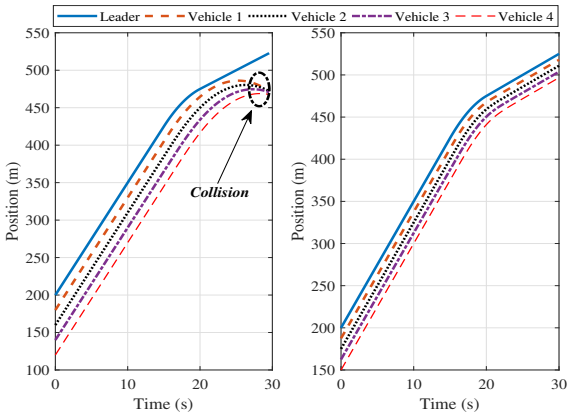

Fig. 3. Position profile for a platoon operating on a wet road, (a). without h dynamics, (b). with h dynamics.

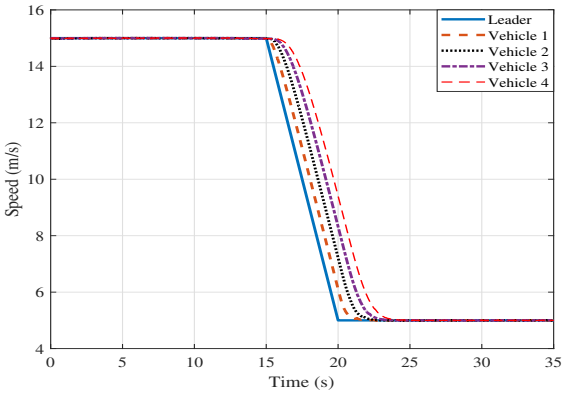

Fig. 4. Longitudinal speed tracking profile.

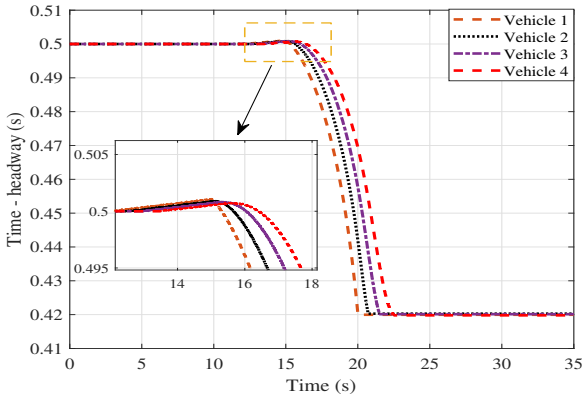

Fig. 5. Time-Headway profile for string stable operation presented in Fig. 4(b).

framework solves this problem by adapting itself to avoid collisions. As shown in Fig. 5, at the instant of braking, the time-headway magnitude in slightly increased. This would in turn increase the desired intervehicular distance ($s_{d_i}(t) = s_o + h_i(t)v_i(t)$), forcing the follower vehicles to instantaneously adjust their positions. This adjustment prevents the vehicles from colliding with each other.

Another important point to note is the fact that the magnitude of the time-headway gets adjusted with speed. With reduction in speed, the magnitude of h becomes smaller, resulting in smaller intervehicular spacing between the vehicles. This reduction in intervehicular spacing is expected to result in reduction in aerodynamic drag, and hence better fuel-efficiency [20].

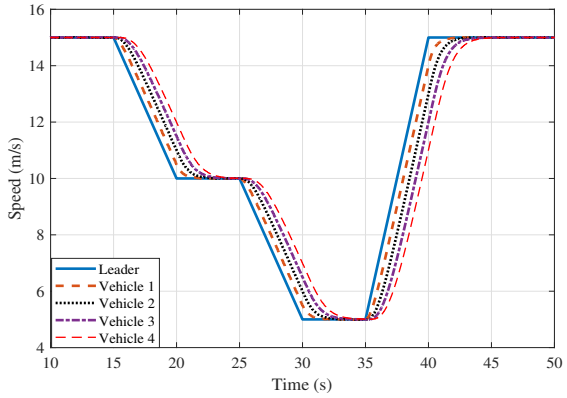

Fig. 6. Leader vehicle speed profile tracking for $\mu = 0.8$.

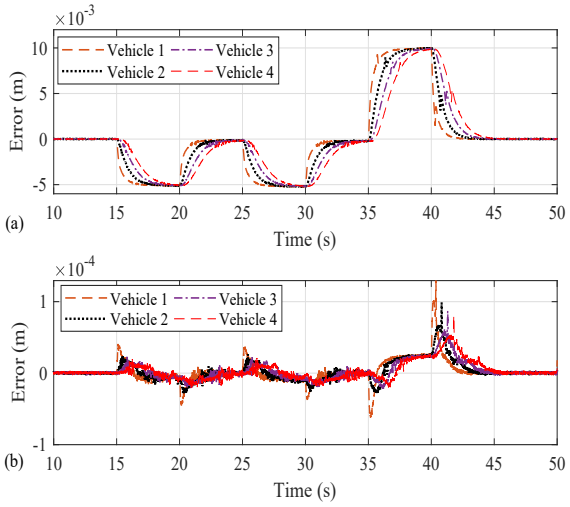

Fig. 7. Instantaneous intervehicular distance error plots; (a). without inclusion of h dynamics, (b). including h dynamics.

To show the importance of including h dynamics in otherwise stable scenarios, the platoon is forced to follow a leader speed profile as shown in Fig. 6. Corresponding follower vehicle speed profiles are also presented in Fig. 6. Both approaches (with and without time-headway dynamics) give similar tracking profiles, courtesy of the APF-based string stable controller. The significance of including h dynamics is presented by comparing the spacing error plots as presented in Fig. 7. Figure 7(a) presents the spacing error plots for CTH approach. The errors are zero at cruising speeds and non-zero during the transient phase. The small

error magnitudes (in the order of millimeters) are by virtue of the APF-based controller used for string stability. If one were to incorporate the h dynamics into the framework, then the instantaneous spacing errors become one order of magnitude lower compared to CTH-based APF controller (as presented in Fig. 7(b)). It is expected that this advantage of the proposed h dynamics-based string stable controller would be carried over when one goes for the practical on-road realization of HCRV platoons.

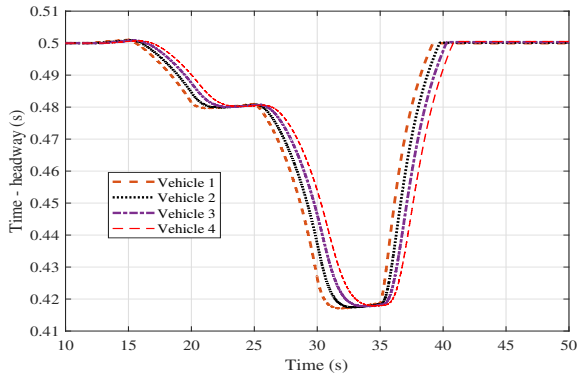

Fig. 8. Time-Headway profile for tracking Fig. 6.

The time-headway generated for tracking the speed profile presented in Fig. 6 is shown in Fig. 8. Starting from $h = 0.5$ s, the time-headway magnitude is varied according to the h dynamics presented in Eq. 14. This variation in time-headway brought the error magnitudes close to zero as presented in Fig. 7(b). The robustness property of APF method when used as a string stable control strategy needs to be analysed further.

VI. Conclusion

A methodology to incorporate time-headway dynamics during string stable controller design for HCRV platoons has been proposed. Through the use of Sliding Mode Control (SMC) technique for deriving time-headway dynamics, a new application of the well established SMC strategy has been explored. The integration of the proposed time-headway dynamics with an Artificial Potential Field (APF)-based string stable controller could ensure stable platoon operation under lead vehicle perturbation maneuvers of high deceleration/acceleration magnitudes on various road conditions. The proposed time-headway dynamics can also be integrated with other well established string stable control techniques to improve their robustness under various operating conditions and perturbations. During the on-road realization of vehicular platoons, the near zero error magnitudes due to the proposed approach would help in meeting the physical actuator constraints, thus making the string stable controller design practically plausible.

Acknowledgements

The authors thank the Ministry of Skill Development and Entrepreneurship, Government of India, for funding through the grant EDD/14-15/023/MOLE/NILE.

References

[1] K.-Y. Liang, J. Mårtensson, and K. H. Johansson, "Heavy-duty vehicle platoon formation for fuel efficiency," *IEEE Transactions on Intelligent Transportation Systems*, vol. 17, no. 4, pp. 1051–1061, 2015.

[2] V. Turri, B. Besselink, and K. H. Johansson, "Cooperative look-ahead control for fuel-efficient and safe heavy-duty vehicle platooning," *IEEE Transactions on Control Systems Technology*, vol. 25, no. 1, pp. 12–28, 2016.

[3] S. W. Smith, Y. Kim, J. Guanetti, R. Li, R. Firoozi, B. Wootton, A. A. Kurzhanskiy, F. Borrelli, R. Horowitz, and M. Arcak, "Improving urban traffic throughput with vehicle platooning: Theory and experiments," *IEEE Access*, vol. 8, pp. 141 208–141 223, 2020.

[4] D. Swaroop and J. K. Hedrick, "String stability of interconnected systems," *IEEE Transactions on Automatic Control*, vol. 41, no. 3, pp. 349–357, 1996.

[5] F. Gao, S. E. Li, Y. Zheng, and D. Kum, "Robust control of heterogeneous vehicular platoon with uncertain dynamics and communication delay," *IET Intelligent Transport Systems*, vol. 10, no. 7, pp. 503–513, 2016.

[6] E. van Nunen, J. Reinders, E. Semsar-Kazerooni, and N. Van De Wouw, "String stable model predictive cooperative adaptive cruise control for heterogeneous platoons," *IEEE Transactions on Intelligent Vehicles*, vol. 4, no. 2, pp. 186–196, 2019.

[7] G. J. Naus, R. P. Vugts, J. Ploeg, M. J. van De Molengraft, and M. Steinbuch, "String-stable cacc design and experimental validation: A frequency-domain approach," *IEEE Transactions on vehicular technology*, vol. 59, no. 9, pp. 4268–4279, 2010.

[8] X. Guo, J. Wang, F. Liao, and R. S. H. Teo, "Distributed adaptive integrated-sliding-mode controller synthesis for string stability of vehicle platoons," *IEEE Transactions on Intelligent Transportation Systems*, vol. 17, no. 9, pp. 2419–2429, 2016.

[9] D. Chen, S. Ahn, M. Chitturi, and D. Noyce, "Truck platooning on uphill grades under cooperative adaptive cruise control (cacc)," *Transportation research part C: emerging technologies*, vol. 94, pp. 50–66, 2018.

[10] K. B. Devika, G. Rohith, V. R. S. Yellapantula, and S. C. Subramanian, "A dynamics-based adaptive string stable controller for connected heavy road vehicle platoon safety," *IEEE Access*, vol. 8, pp. 209 886–209 903, 2020.

[11] K. B. Devika, N. Sridhar, H. Patil, and S. C. Subramanian, "Delay compensated pneumatic brake controller for heavy road vehicle active safety systems," *Proceedings of the Institution of Mechanical Engineers, Part C: Journal of Mechanical Engineering Science*, p. 0954406220952822, 2020.

[12] K. B. Devika, G. Rohith, and S. C. Subramanian, "String stable control of electric heavy vehicle platoon with varying battery pack locations," *Journal of Vibration and Control*, p. 10775463211002619, 2021.

[13] K. B. Devika and S. Thomas, "Power rate exponential reaching law for enhanced performance of sliding mode control," *International Journal of Control, Automation and Systems*, vol. 15, no. 6, pp. 2636–2645, 2017.

[14] G. Rohith, "Fractional power rate reaching law for augmented sliding mode performance," *Journal of the Franklin Institute*, vol. 358, no. 1, pp. 856–876, 2021.

[15] R. Rajamani, *Vehicle dynamics and control*. Springer Science & Business Media, 2011.

[16] H. Pacejka, *Tire and vehicle dynamics*. Elsevier, 2005.

[17] N. Sridhar, K. V. Subramaniyam, S. C. Subramanian, G. Vivekanandan, and S. Sivaram, "Model based control of heavy road vehicle brakes for active safety applications," in *2017 14th IEEE India Council International Conference (INDICON)*. IEEE, 2017, pp. 1–6.

[18] L. Davis, "Stability of adaptive cruise control systems taking account of vehicle response time and delay," *Physics Letters A*, vol. 376, no. 40-41, pp. 2658–2662, 2012.

[19] O. Khatib, "Real-time obstacle avoidance for manipulators and mobile robots," in *Autonomous robot vehicles*. Springer, 1986, pp. 396–404.

[20] A. A. Hussein and H. A. Rakha, "Vehicle platooning impact on drag coefficients and energy/fuel saving implications," *arXiv preprint arXiv:2001.00560*, 2020.